REPORT

Heterozygous Variants in the Mechanosensitive Ion Channel *TMEM63A* Result in Transient Hypomyelination during Infancy

Huifang Yan,[1,2,3,21] Guy Helman,[4,5,21] Swetha E. Murthy,[6] Haoran Ji,[1,7] Joanna Crawford,[5] Thomas Kubisiak,[2] Stephen J. Bent,[8] Jiangxi Xiao,[9] Ryan J. Taft,[10] Adam Coombs,[6] Ye Wu,[1] Ana Pop,[11,12] Dongxiao Li,[1,13] Linda S. de Vries,[14,15] Yuwu Jiang,[1,16] Gajja S. Salomons,[11,12,17,18] Marjo S. van der Knaap,[18,19] Ardem Patapoutian,[6] Cas Simons,[4,5,22] Margit Burmeister,[2,20,22] Jingmin Wang,[1,3,16,22] and Nicole I. Wolf[18,22,*]

Mechanically activated (MA) ion channels convert physical forces into electrical signals. Despite the importance of this function, the involvement of mechanosensitive ion channels in human disease is poorly understood. Here we report heterozygous missense mutations in the gene encoding the MA ion channel TMEM63A that result in an infantile disorder resembling a hypomyelinating leukodystrophy. Four unrelated individuals presented with congenital nystagmus, motor delay, and deficient myelination on serial scans in infancy, prompting the diagnosis of Pelizaeus-Merzbacher (like) disease. Genomic sequencing revealed that all four individuals carry heterozygous missense variants in the pore-forming domain of TMEM63A. These variants were confirmed to have arisen *de novo* in three of the four individuals. While the physiological role of TMEM63A is incompletely understood, it is highly expressed in oligodendrocytes and it has recently been shown to be a MA ion channel. Using patch clamp electrophysiology, we demonstrated that each of the modeled variants result in strongly attenuated stretch-activated currents when expressed in naive cells. Unexpectedly, the clinical evolution of all four individuals has been surprisingly favorable, with substantial improvements in neurological signs and developmental progression. In the three individuals with follow-up scans after 4 years of age, the myelin deficit had almost completely resolved. Our results suggest a previously unappreciated role for mechanosensitive ion channels in myelin development.

Leukodystrophies are genetic disorders primarily affecting brain white matter characterized by the abnormalities they demonstrate on magnetic resonance imaging (MRI).[1–6] MRI pattern recognition often helps to obtain an MRI-based diagnosis in leukodystrophies and enables targeted genetic testing,[7,8] but genetic heterogeneity may require a more comprehensive approach. Next generation sequencing (NGS) has rapidly improved the diagnosis of previously elusive or novel phenotypes with whole-exome sequencing (WES) and whole-genome sequencing (WGS) now directly responsible for implicating a large number of genes with leukodystrophies, greatly reducing the number of unsolved cases.[2,9–12]

Myelination is a protracted developmental process that progresses in infancy following a fixed pattern and is almost complete by the age of 24 months. It can be followed using serial MRI scans.[4,13] A severe deficit of myelin observed on time-separated scans is classified as a hypomyelinating leukodystrophy, a large and genetically heterogeneous group among the leukodystrophies.[14] Clinical presentation is often in early infancy with nystagmus and axial hypotonia, evolving to ataxia and spasticity, with motor development more affected than cognitive function. Alternatively, presentation later in life with a milder clinical picture is also possible.[15,16] The prototype of hypomyelinating leukodystrophies is Pelizaeus-Merzbacher

[1]Department of Pediatrics, Beijing Key Laboratory of Molecular Diagnosis and Study on Pediatric Genetic Diseases, Peking University First Hospital, Beijing 100871, China; [2]Molecular & Behavioral Neuroscience Institute, University of Michigan, Ann Arbor, MI 48109, USA; [3]Joint International Research Center of Translational and Clinical Research, Beijing 100871, China; [4]Murdoch Children's Research Institute, The Royal Children's Hospital, Parkville, Melbourne, VIC 3052, Australia; [5]Institute for Molecular Bioscience, The University of Queensland, Brisbane, QLD 4072, Australia; [6]Howard Hughes Medical Institute, Department of Neuroscience, Dorris Neuroscience Center, Scripps Research, La Jolla, CA 92037 USA; [7]Children's Hospital of Zhejiang University School of Medicine, Hangzhou 310058, China; [8]Data61, Commonwealth Scientific and Industrial Research Organisation, Brisbane, QLD 4067, Australia; [9]Department of Radiology, Peking University First Hospital, Beijing 100871, China; [10]Illumina, Inc., San Diego, CA 92121, USA; [11]Metabolic Unit, Department of Clinical Chemistry, Amsterdam University Medical Centers, Vrije Universiteit, Amsterdam 1081 HV, the Netherlands; [12]Amsterdam Gastroenterology & Metabolism, Amsterdam University Medical Centers, Amsterdam 1081 HV, the Netherlands; [13]Henan Provincial Key Laboratory of Children's Genetic and Metabolic Diseases, Children's Hospital Affiliated to Zhengzhou University, Zhengzhou 450018, China; [14]Department of Neonatology, Wilhelmina Children's Hospital, University Medical Center Utrecht, Utrecht 3584 EA, the Netherlands; [15]UMC Utrecht Brain Center, Utrecht 3584 CG, the Netherlands; [16]Key Laboratory for Neuroscience, Ministry of Education/National Health and Family Planning Commission, Peking University, Beijing 100871, China; [17]Department of Genetic Metabolic Diseases, Amsterdam University Medical Centers, University of Amsterdam, Amsterdam 1105 AZ, the Netherlands; [18]Department of Child Neurology, Emma Children's Hospital, Amsterdam University Medical Centers, Vrije Universiteit Amsterdam and Amsterdam Neuroscience, Amsterdam 1081 HV, the Netherlands; [19]Department of Functional Genomics, Amsterdam Neuroscience, VU University, Amsterdam 1081 HV, the Netherlands; [20]Departments of Computational Medicine & Bioinformatics, Psychiatry and Human Genetics, University of Michigan, Ann Arbor, MI 48109, USA
[21]These authors contributed equally to this work
[22]These authors contributed equally to this work
*Correspondence: n.wolf@amsterdamumc.nl
https://doi.org/10.1016/j.ajhg.2019.09.011.

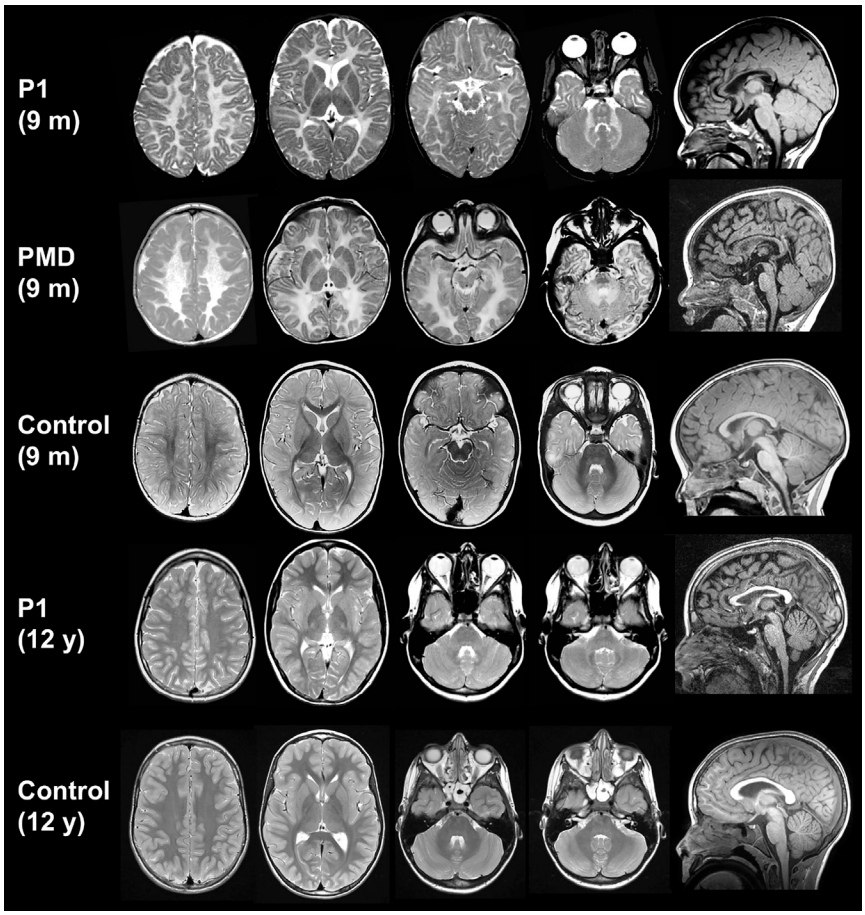

Figure 1. MRI Evolution of Individual 1
Axial T_2-weighted images and a mid-sagittal T_1-weighted image of individual 1 at 9 months and 12 years of age, shown in comparison with age-matched control subjects and an individual with PMD aged 9 months. At 9 months, MRI findings are indistinguishable from PMD, with supra- and infratentorial white matter signal that is diffusely elevated on the T_2-weighted images. The corpus callosum is thinner than normal. At age 12 years, supratentorial white matter signal has normalized, but there is still mild hyperintensity of the cerebellar white matter and the middle cerebellar peduncles.

disease (PMD [MIM: 312080]) due to alterations of *PLP1* (MIM: 300401), encoding the structural myelin protein, proteolipid protein 1.[17] A series of hypomyelinating disorders have been attributed to genetic variants in genes encoding proteins involved in different cellular processes including mRNA translation (tRNA synthetase proteins and cofactors and RNA polymerase III components) and heat-shock response, as well as in genes encoding transcription factors and plasma and lysosomal membrane proteins (please see van der Knaap et al.[6] for a recent comprehensive review).[14] Under the age of 24 months, hypomyelination cannot be diagnosed on MRI with a single exam.[14] However, in the context of profound myelin deficit and a compatible clinical presentation, a hypomyelinating leukodystrophy may be suspected in the first year of life and appropriate investigations can be started. Without a definitive diagnosis, MRI should be repeated to distinguish hypomyelination from delayed myelination.

Here we report on four individuals who presented with a severe myelin deficit observed on serial MRIs, indistinguishable from PMD in the infantile stage (Figure 1), which unexpectedly resolved on follow-up scans, with parallel clinical improvement. Families 1 and 2 were investigated as part of an on-going study on the Amsterdam Database of Leukoencephalopathies to unravel the genetic cause of unclassified leukodystrophies. Families 3 and 4 were identified in Peking University First Hospital (Beijing, China). Institutional ethics approval was granted at both participating centers and written informed consent was secured from the guardians of these individuals. WGS and WES were performed on family trios (proband, biological mother, and biological father) for families 1 and 2 and for families 3 and 4, respectively.

Individual 1 is a 21-year-old male of European descent who was born at term without complications after an uneventful pregnancy. At age 2 weeks, parents noted a pendular nystagmus, increasing with fixation and when agitated. At the age of 2 months, he was an alert baby who could follow objects, but had a tendency toward opisthotonus. In the following months, his development slowly progressed, but at age 8 months, he was not able to sit because of poor balance and had head titubation. He could not grasp objects well due to intention tremor and dysmetria. He could move around by rolling over. His nystagmus had persisted and was now fast. Brain MRI at age 9.5 months showed severe myelin deficit, with no normal myelin signal of both supra- and infratentorial white matter at T_1- and T_2-weighed images (Figures 1 and 2). At 1 year of age, he was able to sit relatively stable and started to pull himself up. Language development was normal. He walked without support at age 20 months. At 5 years, neurological examination showed only mild ataxia; his nystagmus had almost disappeared. He had low vision and mild myopia. Fundoscopy was normal. At age 7 years, he had an episode of vertigo, without nystagmus. Both brain CT and CSF testing (opening pressure, cell count, protein, and glucose) were normal, and vertigo improved within 2 to 3 weeks. At 12 years of age, brain MRI showed normal myelin signal with the exception of the middle cerebellar peduncles and the cerebellar white matter, which were mildly T_2 hyperintense (Figure 1). At age 13 years, he had very mild ataxia with suboptimal tandem

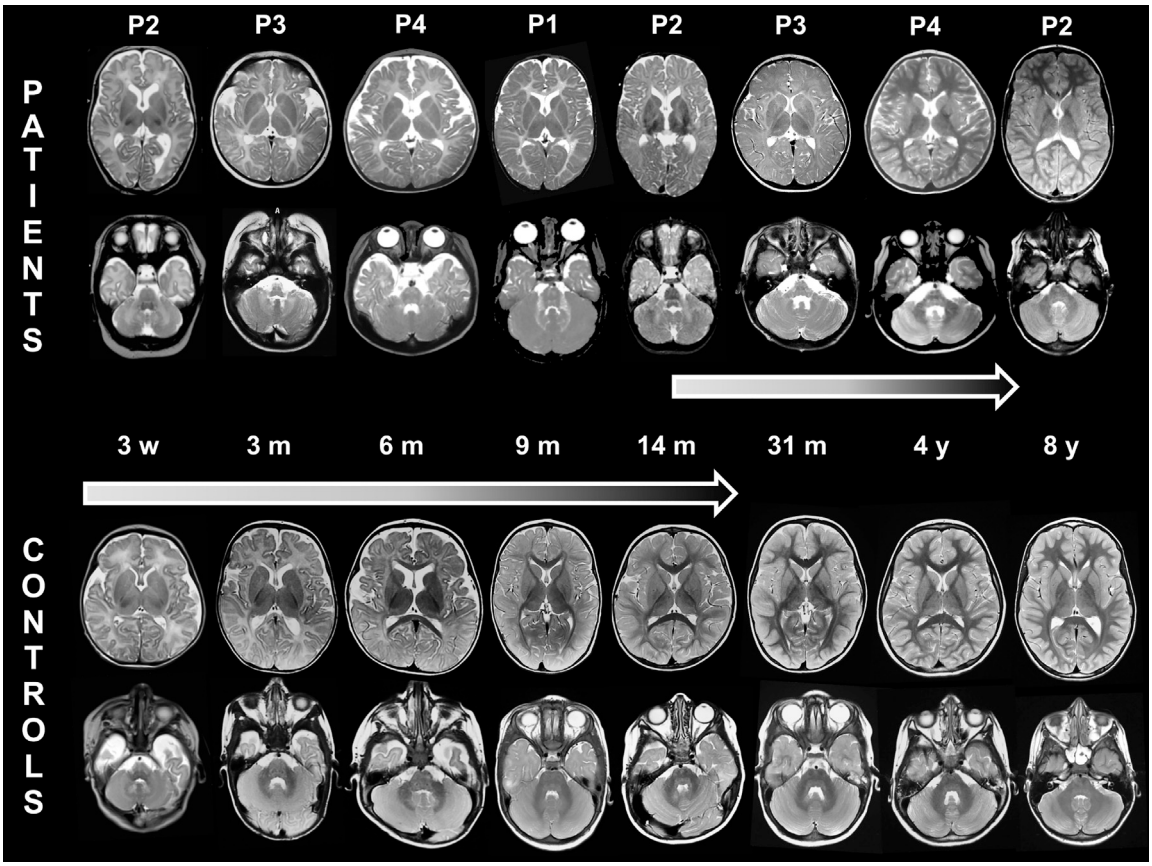

Figure 2. Transient Hypomyelination in Individuals with *TMEM63A* Variants
Serial MRIs (axial T_2-weighted images) of the 4 individuals, from age 3 weeks (left) to age 4 years (right), alongside corresponding images of age-matched healthy children. The normal images of individual 2 at age 8 years and the MRI of individual 1 at age 12 years (see also Figure 1 for this individual) are not depicted here. Myelination shows small improvements only at age 31 months and is completed by age 4 years, whereas it is continually progressing in healthy children, to be virtually completed at age 2 years.

gait and standing on one leg. By age 16 years, he had developed optic atrophy. At that age, he developed Crohn disease, which is stable with treatment. Without cognitive problems, he visited regular school and is now a student at university.

Individual 2 is a 17-year-old male of European descent born at 38 weeks gestational age after a pregnancy complicated by diabetes mellitus treated with insulin. Delivery was by vacuum extraction, and birth weight was 4,700 g. Immediately post-partum, he had to be resuscitated (Apgar scores 1/1/1) but was not intubated. Umbilical cord pH was above 7.20; capillary pH 20 min post-partum was 6.93 with a base excess of −20. On day 2 of life, he developed epileptic seizures, necessitating treatment and artificial ventilation. Brain ultrasound was repeatedly normal. After 1 week, he was seizure-free and discharged at age 2 weeks. Brain MRI at age 3 weeks showed no evidence of hypoxia-related brain lesions, but the normal myelin signal in the posterior limb of the internal capsule (PLIC) was absent (Figure 2). He received antiepileptic treatment during 3 months. Although abnormal brain-stem auditory evoked potentials (BAEP) were observed, his parents thought his hearing was fine. He was first seen in clinic at 4 months, where a pendular nystagmus was noted, accompanied by low axial muscle tone and poor head control with titubation. At age 14 months, brain MRI showed diffuse T_2-hyperintense signal of both supra- and infratentorial white matter (Figure 2). His development slowly progressed, and he was able to walk without support at age 17 months. Language development was slightly delayed. At age 7 years, he had mild gait and appendicular ataxia. His nystagmus had resolved. He went to regular school, but mild learning difficulties became increasingly evident. His IQ was 87 at age 7 years. At 8 years, MRI revealed resolution of hypomyelination. In addition, he had hypospadia corrected at age 8 months and persistent ductus arteriosus, closed at age 18 months. On examination, he lacks several teeth and has mild myopia. Family history was significant for both parents and several siblings. His mother has diabetes mellitus. His father died at age 60 years from a brain tumor. The father's vision was good, and it is not known whether he had nystagmus or delayed development in early life. Five older siblings of the affected individual in this family all declined genetic testing. Two brothers have mild cognitive problems, one sister has diabetes mellitus type I, and the other two sisters are healthy. Two of the older siblings' children, now 2 and 5 years of age, had transient nystagmus, which was not further investigated.

Individual 3 is a 5-year-old female and the second child of an unrelated Chinese couple and has a healthy older sister. Pregnancy and delivery were uneventful. Her birth weight was 3,050 g. Nystagmus was observed 10 days after birth and had resolved by the end of the first year of life. Motor developmental delay was first noted at age 7 months when she still could not hold her head. Gesell development scale (Chinese version) assessed at 7 months showed mild development delay (developmental quotient = 71, individual domain scores were not available in the medical record). She started to walk without support at age 26 months. Currently, she is able to run and jump, but falls easily. Compared to her motor abilities, cognitive development was relatively spared. She started to smile socially at age 2 months and recognized relatives by 4 months. Language expression and understanding were normal, but her pronunciation was suboptimal. With continuous improvement and no regression, she attended regular preschool with normal performance. Hearing and vision were clinically intact. Physical examination performed at 7 months of age demonstrated only mild hypotonia. Brain MRI performed at 3 and 31 months of age implied diffuse myelin deficit in both the supra- and infratentorial brain white matter (Figure 2), compatible with a hypomyelinating leukodystrophy.

Individual 4, now 4 years old, is the second child of unrelated Chinese parents. He was born uneventfully at term by elective cesarean section. His birth weight was 3,600 g. Physiological jaundice was observed and spontaneously subsided after 1 month. Nystagmus was noted after birth and resolved by 14 months of age. At the age of 6 months, vision was decreased and myopia was diagnosed. Fundoscopy was normal. Visual evoked potentials (VEP) performed at ages 6 and 49 months were delayed. His motor development was delayed, with some catching up after the first year of life. Head control was achieved at age 10 months, sitting without support at age 16 months, standing on his own at age 24 months, and walking without support at age 36 months. He started to speak at age 39 months and currently is able to speak long sentences, but with unclear pronunciation. Gesell development scale (Chinese version) assessed at ages 6 months, 17 months, and 50 months showed variable impairment in all domains of development. On follow-up he had made developmental gains. His hearing was clinically normal, though BAEP performed at age 6 months and 49 months had demonstrated delayed conduction of binaural listening pathways in the brainstem and increased hearing thresholds. Myopia was still present. Brain MRI performed at age 6 months and 13 months showed diffuse myelin deficit in the cerebral white matter, which had resolved at age 50 months (Figure 2).

In all of these individuals, results of routine investigations and metabolic testing were normal. PMD was suspected clinically, but *PLP1* dosage was normal as were targeted NGS of 115 leukodystrophy-related genes (including *GJC2* [MIM: 608803]) or individual sequencing of *POLR3A* (MIM: 614258)/*POLR3B* (MIM: 614366) in individual 2. Complete case descriptions are available in the Supplemental Note.

The earliest MRI in our cohort was performed at age 3 weeks in individual 2. The earliest MRIs for all affected individuals, in contrast to healthy age-matched individuals, showed no myelin signal in the posterior limb of the internal capsule (PLIC) (Figure 2). There was no progression of myelination in the ensuing months on T_2-weighted images with diffuse T_2-hyperintense signal of both supra- and infratentorial white matter, including T_2-hyperintense white matter in the cerebellum and the pyramidal tracts and medial lemniscus in the brain stem (Figure 2), in contrast to control subjects where these structures are myelinated as early as 3 months (Figure 2). Myelination had progressed slightly at 14 months (individual 2, Figure 2) when the PLIC, the genu of the corpus callosum, and the frontal periventricular white matter developed a signal isointense with the cortex on T_2-weighted images and the cerebellar white matter became almost isointense with the cerebellar cortex. Myelination had normalized in 3 out of 4 individuals, the earliest by 4 years (individual 4, Figure 2), while individual 3 has not had any indications for a follow-up imaging exam. The last MRI available at 12 years (individual 1) showed mildly T_2-hyperintense signal of the cerebellar white matter and the cerebellar peduncles, reflecting (permanent) white matter involvement (Figure 1).

In two independent studies, NGS detected heterozygous missense variants in Transmembrane Protein 63A (*TMEM63A*; GenBank: NM_014698.2) in each of the four families, including one recurrent variant. The candidate gene was posted on GeneMatcher.[18] *De novo* variants were identified in individual 1 (c.1699G>A [p.Gly567Ser]), individual 3 (c.1385T>A [p.Ile462Asn]), and individual 4 (c.503G>A [p.Gly168Glu]). Individual 2 shared the same variant as individual 1 (c.1699G>A [p.Gly567Ser]), but in this case it was found to be paternally inherited. The father of individual 2 is deceased and records from his childhood were unavailable to determine possible clinical similarities in the infantile period. Individual 2 was also found to have compound heterozygous missense variants in *SLC6A9* (MIM: 601019), encoding a glycine transporter, that were initially investigated as candidates. However, glycine uptake assays performed by overexpression of variant and wild-type constructs in a HEK293-kidney cell line indicated that these variants did not have an obvious impact on transporter activity (results not shown), excluding these variants as candidate pathogenic alleles. Individual 4 also has a single *de novo* variant (c.1936G>A [p.Ala646Thr]) in *GRIA1* (GenBank: NM_001258022.1; MIM: 138248). This variant has been reported in multiple individuals with intellectual disability without MRI abnormalities.[19,20] Interestingly, milestone achievement was more severely delayed in individual 4 (Table 1). Therefore, we suspect that variants in *TMEM63A* and *GRIA1* may both contribute to his phenotype. No other candidate variants emerged from the genomic analysis of these individuals.

Table 1. Clinical Characteristics

Individual	1	2	3	4
Variant	Gly567Ser	Gly567Ser	Ile462Asn	Gly168Glu
Gender	male	male	female	male
Current age	21Y	18Y	5Y	4Y
Age at last assessment	14Y	17Y	5Y	4Y
Nystagmus				
Age at onset	14D	1D	10 D	1D
Age resolved	5Y	7Y	12M	14M
Development				
Walking without support	20M	17M	26M	36M
Language development	normal	slightly delayed	normal	delayed
MRI				
Myelin deficit (age)	9.5M	21D, 14M	3M, 31M	5M, 13M
Myelin normalization (age)	12Y*	8Y*	N/A	4Y*
Myopia	+	+	−	+
Findings at last neurological examination	optic atrophy, mild ataxia	mild ataxia	unclear pronunciation	bilateral Babinski sign, unclear pronunciation
Other	Crohn disease, one self-limiting episode of vertigo	patent ductus arteriosus, hypospadia, abnormal BAEP and VEP	none	abnormal BAEP and VEP
Additional clinically relevant genetic findings	none	none	none	*GRIA1* (NM_001258022.1c.1) c.936G>A (p.Ala646Thr); inheritance: *de novo*

Abbreviations: Y, years; D, days; M, months; N/A, not available; *, earliest exam available; BAEP, brain-stem auditory evoked potential; VEP, visual evoked potential.

The *TMEM63A* variants identified in this study are not present in the 1000 Genomes or gnomAD human population databases and are all predicted to be damaging by multiple prediction tools: SIFT, PolyPhen-2, MutationTaster, M-Cap, Condel, and PROVEAN (Table S1). The three mutated residues are also highly conserved across vertebrate species (Figure 3).

TMEM63A is a member of the OSCA/TMEM63 family of mechanically activated ion channels that are conserved across eukaryotes.[23] In addition to *TMEM63A*, the human genome contains two other members of gene family, *TMEM63B* and *TMEM63C*. To date, neither *TMEM63A* or its two paralogs have been associated with human disease. *TMEM63A* is highly expressed in oligodendrocytes and mouse *Tmem63a* shows significantly higher expression in myelinating oligodendrocytes and in microglia (Brain RNA-seq database) . The International Mouse Phenotyping Consortium (IMPC) database reports a small but significant proportion of *Tmem63a*-null mice demonstrate gait abnormalities.

Using a cryo-EM structure of the TMEM63A homolog OSCA1.2 from *Arabidopsis*, we generated a model of TMEM63A protein structure using SWISS-MODEL (Figure 3B).[21,22] The Gly168 residue sits in an intracellular loop between helix 1 and helix 2 while both Ile462 and Gly567 are located within pore lining transmembrane helices of TMEM63A. Interestingly Gly567 resides on the internal face of the pore one helix turn from the conserved residue Glu571 that has been shown to reduce stretch activated ion conductance when mutated to alanine in OSCA1.2.[21]

We introduced the variants seen in these individuals by site directed mutagenesis into TMEM63A clones purchased from Origene (GenBank: NM_014698, Cat No.: RC206992). Wild-type and mutant constructs were subcloned into an IRES_mCherry vector and transfected into PIEZO1-knockout Human Embryonic Kidney 293T cells. Using a previously described cell-based stretch-activated channel activity assay,[21,23] we characterized the impact of each of the three variants on TMEM63A channel activity (Figure 4). Mechanical stimulation, induced by the application of negative pressure in the recording electrode, elicited stretch-activated currents in cells transfected with wild-type TMEM63A. However, cells transfected with each of the three *TMEM63A* variants (Gly168Glu: n = 7; Ile462Asn n = 9; Gly567Ser: n = 7) failed to induce stretch-activated currents (Figure 4B). The assay performed cannot determine whether the observed defect results from a direct effect on channel gating or if it is due to compromised protein folding and trafficking to the cell membrane. In either case, these results strongly suggest that these variants cause a loss of *TMEM63A* function.

The data presented here associate heterozygous variants in *TMEM63A* with a leukodystrophy with transient myelin

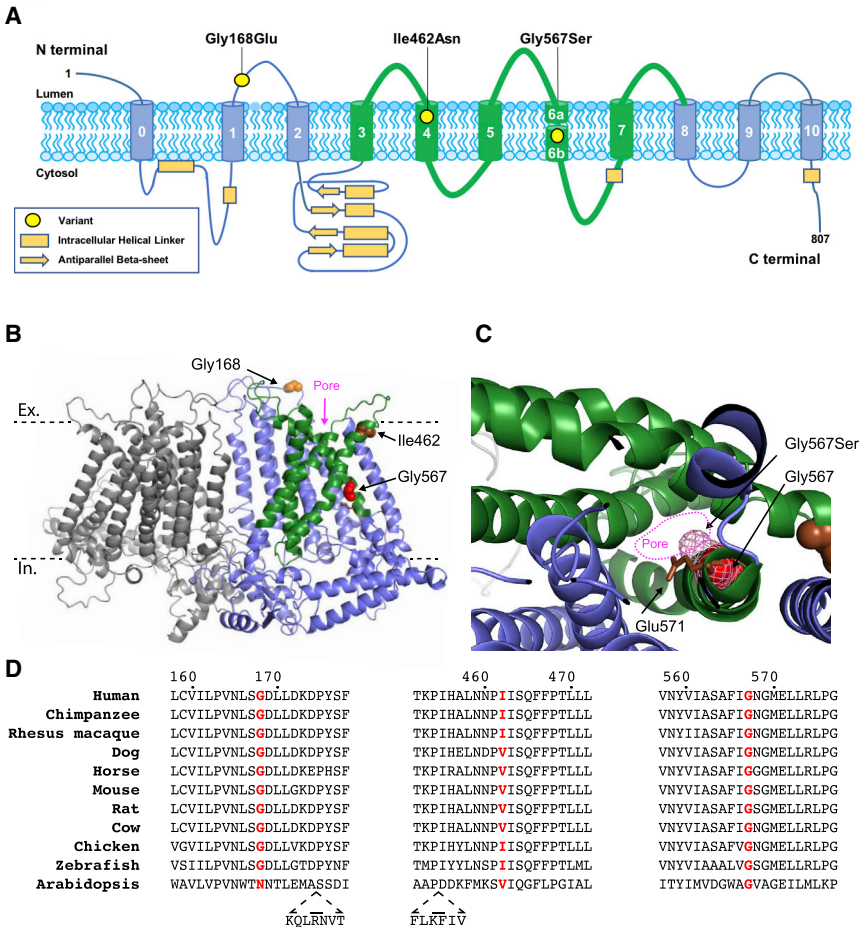

Figure 3. Protein Structure and Variant Conservation

(A) Location of the three identified variants shown on a schematic representation of TMEM63A protein (Uniprot: O94886).

(B and C) Predicted structure TMEM63A protein based on cryo-EM structure of *Arabidopsis* homolog OSCA1.2 (PDB: 6MGV). The model was generated using SWISS-MODEL.[21,22] Residues altered by the variants are shown as spheres. The approximate location of the extracellular (Ex) and intracellular (In) surfaces of plasma membrane are indicated by dashed black lines. The five pore lining transmembrane helices are shown in green.[21]

(C) Section of TMEM63A structural model looking through pore region toward the extracellular domain. The Gly576 residue is shown as red spheres, and pink mesh indicates the predicted position the serine side-chain would occupy in the p.Gly576Ser mutant protein. The conserved residue, Glu571 (shown as brown sticks), that has been shown to reduce stretch activated ion conductance when mutated to alanine in OSCA1.2 can be seen adjacent to Gly576.[21]

(D) Clustal alignment of TMEM63A protein from ten vertebrate species and the *Arabidopsis* homolog OSCA1.2. The residues altered in the presented individuals are highlighted in red.

deficiency during infancy. All four case subjects had clinical presentations suggestive of PMD or PMLD at an early age with nystagmus and delayed motor development and MRIs demonstrating a pattern suggestive of hypomyelination (present on serial MRIs in three individuals and profound myelin deficiency on single MRIs in the other infant). Myopia was present in three individuals, including one who developed optic atrophy. However, clinical evolution in all four individuals has been surprisingly favorable, with resolution of nystagmus, near-normalization of neurological signs, and gains in developmental skills. Two individuals have intellectual disability and had abnormal BAEP testing results, although clinically normal hearing. Concurrent with the improvement in neurological signs, MRI showed unexpected normalization. In two individuals the myelin deficit appears to have completely resolved and in one individual only mild abnormalities persist. The remaining individual, last imaged at 31 months, also displayed improvement of myelination.

The distinction between hypomyelination and delayed myelination can be challenging. PMD is a severe neurologic disorder characterized by hypomyelination with lasting cognitive and motor deficits. Individuals with PMD may achieve small developmental gains but do not acquire sitting without support and demonstrate progressive spasticity and gradual deterioration typically by 10–12 years of age. Delayed myelination can be a non-specific finding across a spectrum of infantile-onset neurologic disorders. Profoundly delayed myelination with slow improvement and even complete resolution of myelin deficiency on MRI has been observed in Allan-Herndon-Dudley syndrome (AHDS [MIM: 300523]), due to variants in *MCT8* (MIM: 300095) encoding a thyroid hormone transporter.[4,24] However, in AHDS, individuals typically remain severely affected, and clinical signs do not improve even when there are radiologic changes that suggest normalization of the myelin deficit.[24,25] Temporally, neither MRI findings nor clinical development were compatible with PMD or AHDS in individuals with variants in *TMEM63A* despite their early presentation, thus we characterized this presentation as a transient myelin deficiency.

TMEM63A, also named CSC1-like protein 1, was initially suggested to be a hyperosmolarity activated ion channel.[26,27] More recently it was demonstrated that TMEM63s are MA ion channels that elicit stretch-activated currents when expressed in naive cells.[23] The results described here clearly demonstrate that each of the hypomyelination associated variants result in a loss of TMEM63A function. This suggests a previously unappreciated role for *TMEM63A* in early myelin development. How disruption of this activity results in the apparently temporary myelin deficit observed in these individuals is unclear. *TMEM63A* has two highly similar homologs, *TMEM63B* and *TMEM63C*. It is possible

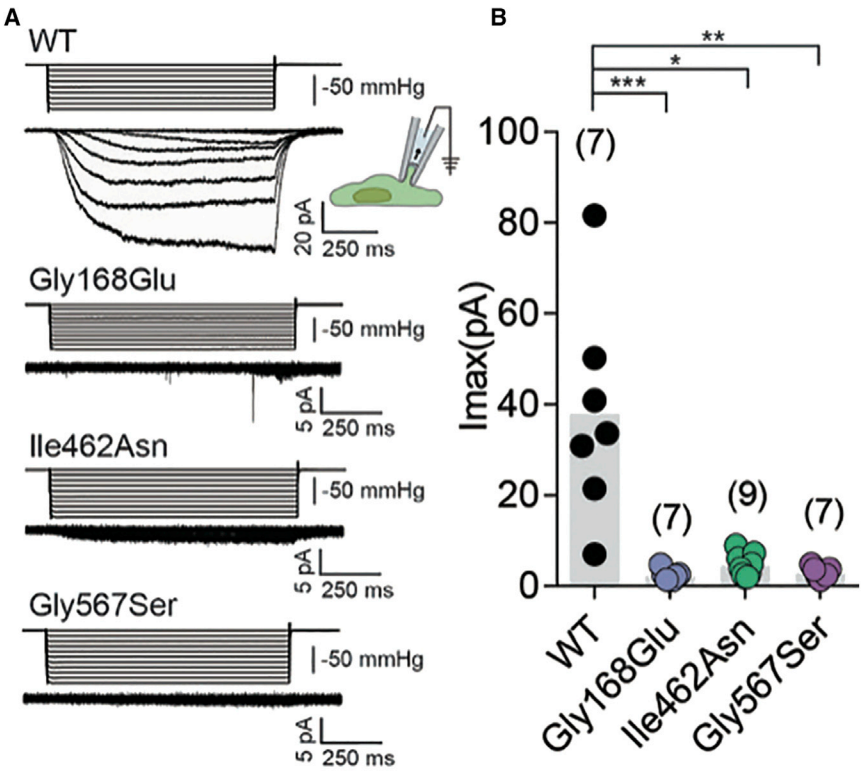

Figure 4. Mutant Constructs Fail to Induce MA Currents in HEK-P1KO Cells

(A) Representative stretch-activated currents induced by negative pipette pressure from cells transfected with wild-type or the indicated mutant construct. Corresponding pressure stimulus is illustrated above the current trace. Vertical scale bar: 50 mmHg.

(B) Maximal stretch-activated currents recorded from cells expressing wild-type TMEM63A (n = 7) or the indicated variant of TMEM63A p.Gly168Glu (n = 7), p.Ile462Asn (n = 9), and p.Gly567Ser (n = 7). ***p = 0.0002, *p = 0.0411, **p = 0.0031, Dunn's multiple comparison test.

that developmental and tissue-specific expression of these homologs provide some compensation for the loss of *TMEM63A* activity.[23]

Finally, our findings add *TMEM63A* to a growing list of leukodystrophies caused by heterozygous variants, the majority of which arise *de novo*. Disorders that arise sporadically are unable to be identified by techniques such as linkage analysis that permit an estimation of a molecular cause of disease. Trio NGS has demonstrated success in these case subjects, with heterozygous variants in *CSF1R* (MIM: 164770), *TUBB4A* (MIM: 602662), and *TMEM106B* (MIM: 613416) found to cause a prominent leukodystrophy.[9,28,29]

Further monitoring of these individuals described in this paper will be necessary to better understand the natural course of the disease related to heterozygous *TMEM63A* variants and to reveal whether there is a risk of slow regression over time. While this disorder resembles classical hypomyelination in infancy, the clinical and radiological normalization in childhood prompts suggestions that this phenotype may be better termed infantile-onset transient hypomyelination. The favorable clinical evolution associated in spite of these damaging variants provides prognostically important information for affected families. It also emphasizes that myelination can evolve normally even when it is initiated later than usual, giving hope for therapeutic trials in hypomyelinating disorders.

Supplemental Data

Supplemental Data can be found online at https://doi.org/10.1016/j.ajhg.2019.09.011.

Acknowledgments

The authors would like to thank the affected individuals and their families. We thank Dr. Truus E.M. Abbink, Carola van Berkel, and Nienke L. Postma for their invaluable assistance.

This work was supported in part by the National Key Research and Development Program of China (No. 2016YFC1306201 and No. 2016YFC0901505). H.Y.'s visit in M.B.'s laboratory was supported by the China Scholarship Council. H.Y. also reports funding from the UMHS-PUHSC Joint Institute for Translational and Clinical Research (BMU2019JI009). The participation of G.H. and C.S. is in part financed by the Australian National Health and Medical Research Council (NHMRC 1068278). The research conducted at the Murdoch Children's Research Institute was supported by the Victorian Government's Operational Infrastructure Support Program. A. Patapoutian is an investigator of the Howard Hughes Medical Institute.

Declaration of Interests

R.J.T. is an employee of Illumina, Inc.; otherwise the authors report no conflicts of interest.

Received: July 4, 2019
Accepted: September 9, 2019
Published: October 3, 2019

Web Resources

Brain RNaseq database, http://www.brainrnaseq.org
GenBank, https://www.ncbi.nlm.nih.gov/genbank/
GeneMatcher, https://genematcher.org/
IMPC, https://www.mousephenotype.org/data/experiments?geneAccession=MGI:2384789

OMIM, https://www.omim.org/
RCSB Protein Data Bank, http://www.rcsb.org/pdb/home/home.do
UniProt, https://www.uniprot.org:443/uniprot/O94886

References

1. van der Knaap, M.S., and Bugiani, M. (2017). Leukodystrophies: a proposed classification system based on pathological changes and pathogenetic mechanisms. Acta Neuropathol. *134*, 351–382.
2. Kevelam, S.H., Steenweg, M.E., Srivastava, S., Helman, G., Naidu, S., Schiffmann, R., Blaser, S., Vanderver, A., Wolf, N.I., and van der Knaap, M.S. (2016). Update on Leukodystrophies: A Historical Perspective and Adapted Definition. Neuropediatrics *47*, 349–354.
3. Vanderver, A., Prust, M., Tonduti, D., Mochel, F., Hussey, H.M., Helman, G., Garbern, J., Eichler, F., Labauge, P., Aubourg, P., et al.; GLIA Consortium (2015). Case definition and classification of leukodystrophies and leukoencephalopathies. Mol. Genet. Metab. *114*, 494–500.
4. van der Knaap, M.S., and Valk, J. (2005). Magnetic Resonance of Myelination and Myelin Disorders (Berlin: Springer).
5. Schiffmann, R., and van der Knaap, M.S. (2004). The latest on leukodystrophies. Curr. Opin. Neurol. *17*, 187–192.
6. van der Knaap, M.S., Schiffmann, R., Mochel, F., and Wolf, N.I. (2019). Diagnosis, prognosis, and treatment of leukodystrophies. Lancet Neurol. *18*, 962–972.
7. Steenweg, M.E., Vanderver, A., Blaser, S., Bizzi, A., de Koning, T.J., Mancini, G.M., van Wieringen, W.N., Barkhof, F., Wolf, N.I., and van der Knaap, M.S. (2010). Magnetic resonance imaging pattern recognition in hypomyelinating disorders. Brain *133*, 2971–2982.
8. Schiffmann, R., and van der Knaap, M.S. (2009). Invited article: an MRI-based approach to the diagnosis of white matter disorders. Neurology *72*, 750–759.
9. Simons, C., Dyment, D., Bent, S.J., Crawford, J., D'Hooghe, M., Kohlschütter, A., Venkateswaran, S., Helman, G., Poll-The, B.T., Makowski, C.C., et al.; Care4Rare Consortium (2017). A recurrent de novo mutation in *TMEM106B* causes hypomyelinating leukodystrophy. Brain *140*, 3105–3111.
10. Vanderver, A., Simons, C., Helman, G., Crawford, J., Wolf, N.I., Bernard, G., Pizzino, A., Schmidt, J.L., Takanohashi, A., Miller, D., et al.; Leukodystrophy Study Group (2016). Whole exome sequencing in patients with white matter abnormalities. Ann. Neurol. *79*, 1031–1037.
11. Dorboz, I., Aiello, C., Simons, C., Stone, R.T., Niceta, M., Elmaleh, M., Abuawad, M., Doummar, D., Bruselles, A., Wolf, N.I., et al. (2017). Biallelic mutations in the homeodomain of NKX6-2 underlie a severe hypomyelinating leukodystrophy. Brain *140*, 2550–2556.
12. Miyake, N., Wolf, N.I., Cayami, F.K., Crawford, J., Bley, A., Bulas, D., Conant, A., Bent, S.J., Gripp, K.W., Hahn, A., et al. (2017). X-linked hypomyelination with spondylometaphyseal dysplasia (H-SMD) associated with mutations in AIFM1. Neurogenetics *18*, 185–194.
13. Barkovich, A.J. (2005). Magnetic resonance techniques in the assessment of myelin and myelination. J. Inherit. Metab. Dis. *28*, 311–343.
14. Pouwels, P.J.W., Vanderver, A., Bernard, G., Wolf, N.I., Dreha-Kulczewksi, S.F., Deoni, S.C.L., Bertini, E., Kohlschütter, A., Richardson, W., Ffrench-Constant, C., et al. (2014). Hypomyelinating leukodystrophies: translational research progress and prospects. Ann. Neurol. *76*, 5–19.
15. Harting, I., Karch, S., Moog, U., Seitz, A., Pouwels, P.J.W., and Wolf, N.I. (2019). Oculodentodigital Dysplasia: A Hypomyelinating Leukodystrophy with a Characteristic MRI Pattern of Brain Stem Involvement. AJNR Am. J. Neuroradiol. *40*, 903–907.
16. Wolf, N.I., Vanderver, A., van Spaendonk, R.M., Schiffmann, R., Brais, B., Bugiani, M., Sistermans, E., Catsman-Berrevoets, C., Kros, J.M., Pinto, P.S., et al.; 4H Research Group (2014). Clinical spectrum of 4H leukodystrophy caused by *POLR3A* and *POLR3B* mutations. Neurology *83*, 1898–1905.
17. Hobson, G.M., and Garbern, J.Y. (2012). Pelizaeus-Merzbacher disease, Pelizaeus-Merzbacher-like disease 1, and related hypomyelinating disorders. Semin. Neurol. *32*, 62–67.
18. Sobreira, N.L.M., Arachchi, H., Buske, O.J., Chong, J.X., Hutton, B., Foreman, J., Schiettecatte, F., Groza, T., Jacobsen, J.O.B., Haendel, M.A., et al. (2017). Matchmaker Exchange. Curr. Protoc. Hum. Genet. *95*, 9.31.1.
19. de Ligt, J., Willemsen, M.H., van Bon, B.W., Kleefstra, T., Yntema, H.G., Kroes, T., Vulto-van Silfhout, A.T., Koolen, D.A., de Vries, P., Gilissen, C., et al. (2012). Diagnostic exome sequencing in persons with severe intellectual disability. N. Engl. J. Med. *367*, 1921–1929.
20. Geisheker, M.R., Heymann, G., Wang, T., Coe, B.P., Turner, T.N., Stessman, H.A.F., Hoekzema, K., Kvarnung, M., Shaw, M., Friend, K., et al. (2017). Hotspots of missense mutation identify neurodevelopmental disorder genes and functional domains. Nat. Neurosci. *20*, 1043–1051.
21. Jojoa-Cruz, S., Saotome, K., Murthy, S.E., Tsui, C.C.A., Sansom, M.S., Patapoutian, A., and Ward, A.B. (2018). Cryo-EM structure of the mechanically activated ion channel OSCA1.2. eLife *7*, e41845.
22. Waterhouse, A., Bertoni, M., Bienert, S., Studer, G., Tauriello, G., Gumienny, R., Heer, F.T., de Beer, T.A.P., Rempfer, C., Bordoli, L., et al. (2018). SWISS-MODEL: homology modelling of protein structures and complexes. Nucleic Acids Res. *46* (W1), W296–W303.
23. Murthy, S.E., Dubin, A.E., Whitwam, T., Jojoa-Cruz, S., Cahalan, S.M., Mousavi, S.A.R., Ward, A.B., and Patapoutian, A. (2018). OSCA/TMEM63 are an Evolutionarily Conserved Family of Mechanically Activated Ion Channels. eLife *7*, e41844.
24. Vaurs-Barrière, C., Deville, M., Sarret, C., Giraud, G., Des Portes, V., Prats-Viñas, J.M., De Michele, G., Dan, B., Brady, A.F., Boespflug-Tanguy, O., and Touraine, R. (2009). Pelizaeus-Merzbacher-Like disease presentation of MCT8 mutated male subjects. Ann. Neurol. *65*, 114–118.
25. Azzolini, S., Nosadini, M., Balzarin, M., Sartori, S., Suppiej, A., Mardari, R., Greggio, N.A., and Toldo, I. (2014). Delayed myelination is not a constant feature of Allan-Herndon-Dudley syndrome: report of a new case and review of the literature. Brain Dev. *36*, 716–720.
26. Hou, C., Tian, W., Kleist, T., He, K., Garcia, V., Bai, F., Hao, Y., Luan, S., and Li, L. (2014). DUF221 proteins are a family of osmosensitive calcium-permeable cation channels conserved across eukaryotes. Cell Res. *24*, 632–635.
27. Zhao, X., Yan, X., Liu, Y., Zhang, P., and Ni, X. (2016). Co-expression of mouse TMEM63A, TMEM63B and TMEM63C

confers hyperosmolarity activated ion currents in HEK293 cells. Cell Biochem. Funct. *34*, 238–241.

28. Simons, C., Wolf, N.I., McNeil, N., Caldovic, L., Devaney, J.M., Takanohashi, A., Crawford, J., Ru, K., Grimmond, S.M., Miller, D., et al. (2013). A de novo mutation in the β-tubulin gene TUBB4A results in the leukoencephalopathy hypomyelination with atrophy of the basal ganglia and cerebellum. Am. J. Hum. Genet. *92*, 767–773.

29. Karle, K.N., Biskup, S., Schüle, R., Schweitzer, K.J., Krüger, R., Bauer, P., Bender, B., Nägele, T., and Schöls, L. (2013). De novo mutations in hereditary diffuse leukoencephalopathy with axonal spheroids (HDLS). Neurology *81*, 2039–2044.